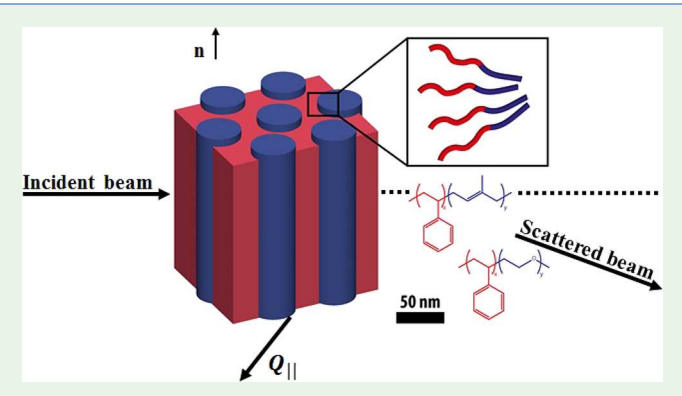
# Nanoscale Q-Resolved Phonon Dynamics in Block Copolymers

Dima Bolmatov,\*<sup>,†,‡</sup> Qi Zhang,<sup>§</sup> Dmytro Soloviov, <sup>||,⊥,#</sup> Yuk Mun Li,<sup>§</sup> Jörg G. Werner, <sup>∇</sup> Alexey Suvorov, Yong Q. Cai, Ulrich Wiesner, Mikhail Zhernenkov, and John Katsaras <sup>†,‡</sup>

ABSTRACT: In recent years, responsive polymer-based structures have been studied extensively due to their unique ability to alter their physical properties upon exposure to external stimuli. Despite this, the nanoscale Q-resolved dynamic properties of these materials have barely been explored, which is limiting the development and applications of these materials. To address this issue, we used inelastic Xray scattering (IXS) and found evidence for van der Waals mediated molecular vibration-responsive rattling dynamics in bulk poly(isoprene-block-styrene) (SI) and poly(styreneblock-ethylene oxide) (SO) stacked thin film block copolymers. Their cylinder-forming hexagonally arranged static structures were characterized using small-angle X-ray scatter-



ing (SAXS) and grazing incidence small-angle X-ray scattering (GISAXS), complemented by scanning electron microscopy (SEM). Specifically, we observed that the longitudinal vibrational mode in bulk SI experiences a strong phonon attenuation as temperature increases from 30 to 90 °C, while the transverse phonon excitations are nonexistent in the measured Q-range due to anharmonicity-mediated symmetry breaking in phonon interactions. Furthermore, the emergent transverse acoustic phonon modes in both the bulk SI and SO thin films exhibited a nondispersive behavior with a nearly zero slope in the hydrodynamic limit  $(Q \to 0)$ , mimicking optical phonon excitations (i.e., standing waves). In summary, these findings point to the use of polymeric materials for Q-resolved nanoacoustic sensing, and the visualization of THz phonons.

KEYWORDS: block copolymers, Q-resolved polymer dynamics, emergent transverse phonons, phonon Q-gap, Q-resolved nanoacoustic polymer sensing

#### INTRODUCTION

The use of complementary experimental techniques with nanoscale precision has grown dramatically in the study of soft complex and hybrid materials. 1-9 Interest in understanding the dynamic and static properties of such materials is steadily increasing due to their potential applications as smart materials for sensing and bioinspired applications. 10-15 Currently, polymer-based stimuli-responsive materials are at the leading edge of materials science research due to their ability to alter their functionalities as a result of external stimuli. 16-18 For example, they can control ion, molecule, and heat transfer; convert biochemical signals into optical, electrical, thermal, and mechanical signals; and play a major role in drug delivery, tissue engineering, biosensors, actuators, smart textiles, and fibers. 19-32 Recent developments in polymer synthesis have

produced macromolecular structures precisely engineered at the molecular level, <sup>33–36</sup> which have the potential to revolutionize this field of study and enable the search for emerging functionalities at the nanoscale.

Heat transfer and energy conversion in soft materials are mainly governed by thermal conduction, where phonon (quantized elastic waves) propagation plays a key role. 37-50 In this regard, sound waves and phonon propagation in polymerbased materials represent a rapidly developing field to be explored at different time and length scales. 51-60 Weak interchain van der Waals and strong intrachain covalent bonds

Received: June 28, 2018 Accepted: September 4, 2018 Published: September 4, 2018



<sup>&</sup>lt;sup>†</sup>Neutron Scattering Division, Oak Ridge National Laboratory, Oak Ridge, Tennessee 37831, United States

<sup>&</sup>lt;sup>‡</sup>Department of Physics and Astronomy, University of Tennessee, Knoxville, Tennessee 37996, United States

<sup>§</sup>Department of Materials Science and Engineering, Cornell University, Ithaca, New York 14850, United States

Frank Laboratory of Neutron Physics, Joint Institute for Nuclear Research, Dubna 141980, Russia

<sup>&</sup>lt;sup>1</sup>Taras Shevchenko National University of Kyiv, Kyiv 01033, Ukraine

<sup>\*</sup>Moscow Institute of Physics and Technology, Dolgoprudny 141701, Russia

 $<sup>^{</sup>abla}$ School of Engineering and Applied Sciences and Department of Physics, Harvard University, Cambridge, Massachusetts 02138, United States

ONational Synchrotron Light Source II, Brookhaven National Laboratory, Upton, New York 11973, United States

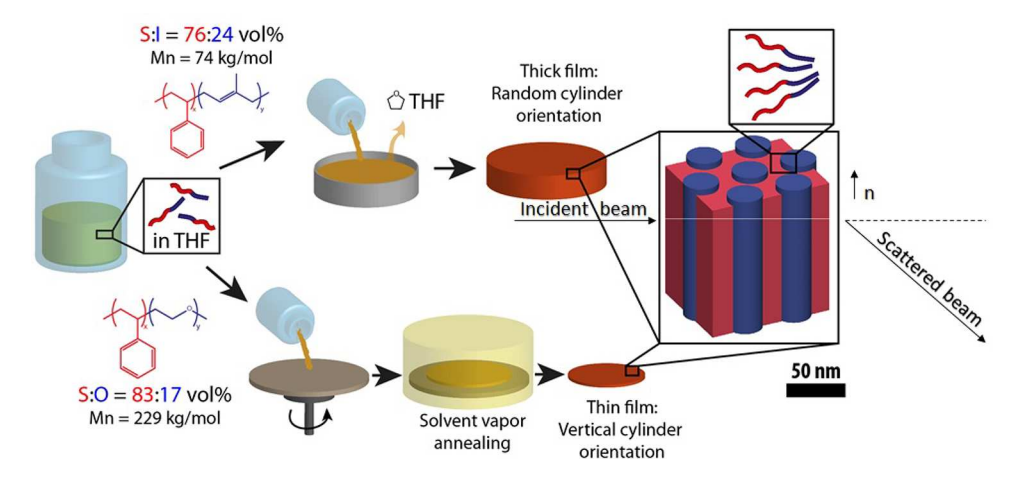


**Figure 1.** Schematic illustrating block copolymer film fabrication. The SI bulk sample most likely consists of "grains" with random orientation of hexagonally arranged cylinders between different grains. The X-ray probes many different orientations of the cylinders at the same time. In the case of SO thin films, cylinders are aligned along the film normal with solvent annealing; hence, both structure and phonon dynamics of SO samples were studied in the plane orthogonal to hexagonally arranged cylinders.

represent two important types of molecular interactions in polymers. For example, the intrachain collective vibrations get activated at relatively high energies (200-300 meV) due to bending, rocking, symmetric and asymmetric stretching, wagging, and twisting experienced by the C-H and C-C bonds in the backbone polymer chains.<sup>61</sup> The existence of transverse phonon excitations in polymer-based materials has previously been observed at GHz frequencies, 62 including the recent discovery of shear bands at Hz frequencies. 63 However, it is not clear whether or not these materials are capable of propagating shear elastic waves at sub- and THz-frequencies (sub- and meV-energies).<sup>64</sup> Despite numerous attempts, the low-energy Q-resolved (momentum-resolved) van der Waals mediated phonon dynamics (1-8 meV) in polymeric materials have not been studied at the nanoscale, with the exception of a single longitudinal phonon mode.<sup>64</sup> Importantly, experimental evidence for the acoustic transverse van der Waals mediated collective excitations remains elusive, and is thought to limit the further development of polymer-based materials operating at nanometer-THz scales.

Here, we report on the interchain van der Waals mediated nanoscale collective dynamics in bulk SI and SO stacked thin film block copolymers probed by Q-resolved high-spectral contrast inelastic X-ray scattering (IXS) in the frequency range 0.24-1.93 THz. The two polymer samples [poly(isopreneblock-styrene) (SI) and poly(styrene-block-ethylene oxide) (SO)] were chosen because of their different chemical and physical nature regarding the cylinder phase. While both cylinder-forming block copolymers have a polystyrene matrix that is in its glassy state at room temperature, they differ in the block that forms the one-dimensional cylinder. The SI cylinders are made of the "squishy" polyisoprene, while the SO cylinders are made of the semicrystalline poly(ethylene oxide). The red matrix (see Figure 1) in both samples is polystyrene (PS or simply "S"), which has a glass transition temperature,  $T_g$ , around 100 °C. However, in block copolymers, the glass transition of polystyrene is often suppressed to around 95-100 °C, in particular when blocked with low- $T_{\rm g}$  materials, like polyisoprene. In the case of SI, the blue cylinders (see Figure 1) are polyisoprene (PI or simply "I") with a glass transition temperature around -60 °C. For SO, the blue cylinders are poly(ethylene oxide) (PEO or simply "O") with a glass

transition of about -50 °C and a melting point of around 40 °C. Furthermore, in the case of the SO thin films, we were able to obtain aligned cylinders along the film normal with solvent annealing, which we believe may contain interesting anisotropic effects affecting their acoustic properties, something that we will explore in the future.

The static structures of both samples were characterized through SAXS and grazing incidence SAXS (GISAXS) measurements, respectively, and complemented with SEM images. The SI bulk sample most likely consists of "grains" with random orientation of the hexagonally arranged cylinders between different grains. Overall, in the SI bulk film X-rays probe the different orientations of the cylinders simultaneously. In the case of the SO thin films, both structure and phonon dynamics of these polymer samples have been studied in the plane orthogonal to the hexagonally arranged cylinders, see Figure 1. Specifically, we observed a significant change in the phonon landscape of the SI bulk sample with temperature increase. The longitudinal vibrational mode experienced a strong phonon attenuation when the temperature was raised from 30 to 90 °C. At the same time, the transverse mode became fully overdamped at 90 °C as a result of anharmonicity-mediated symmetry breaking in phonon interactions. Finally, the transverse acoustic modes in both bulk SI and SO thin films exhibited nondispersive phonon features upon approaching the hydrodynamic limit (Q  $\rightarrow$  0) resembling the so-called breathing modes in the form of standing waves. Finally, the importance of further Q-resolved phonon dynamics studies of polymer-based materials is also discussed.

## RESULTS AND DISCUSSION

It is possible that one day thermally conductive polymer-based materials can be used to substitute conventional plastics, ceramics, and even metals, as heat-transfer materials. Currently, however, bulk polymers usually have low thermal conductivity due to the presence of defects such as polymer chain ends, entanglement, random orientation, voids, and impurities. Impurities act as stress concentrators affecting phonon propagation and, as a result, heat transfer. Incorporating a second polymer that is covalently tethered to the first (a polymer matrix) enhances the material's thermal conductivity due to thermal resistance between the two polymers. <sup>65</sup> As a result, the

study of phonon dynamics in block copolymers is thought to be a promising path of research.

Block Copolymer Bulk Measurements. Synthesis of Poly(isoprene-block-styrene) (SI) Polymerization. Benzene solvent was first distilled into a reactor placed in a glovebox, and the anionic initiator, sec-butyllithium (Sigma-Aldrich), was added to the reactor with a syringe. Isoprene was distilled over *n*butyllithium (Sigma-Aldrich), added to the reactor, and allowed to polymerize. After 8 h, styrene distilled over di-nbutylmagnesium (Sigma-Aldrich) was also added to the reactor. The styrene was polymerized onto the polyisoprene block overnight, and polymerization was terminated using degassed methanol. The final block copolymer was dissolved in chloroform and precipitated into methanol. Polymer properties are listed in Table 1, where  $M_n$  is the number-average molecular

Table 1. SI Bulk and SO Thin Film Block Copolymer Physical **Properties** 

polymer	$M_{\rm n}$ (kg/mol)	$f_{\rm PI}$ (vol %)	$f_{PS}$ (vol %)	$f_{\rm PEO}~({ m vol}~\%)$	PDI
SI	74	24	76		1.04
SO	229		83	17	1.10

weight,  $f_{PI}$  (vol %) is the volume fraction of poly(isoprene),  $f_{PS}$ (vol %) is the volume fraction of poly(styrene),  $f_{PEO}$  (vol %) is the volume fraction of poly(ethylene oxide), and PDI is the polydispersity index (measure of the polymer's molecular weight polydispersity).

Sample Preparation. In Figure 1 we demonstrate the scheme illustration for block copolymer film fabrication. The bulk SI sample was prepared through evaporation-induced selfassembly (EISA). A 5 wt % SI solution in tetrahydrofuran (THF) was added into a small Teflon beaker and heated on a hot plate to 50 °C until the solvent was dried of. A glass dome was used to cover the Teflon beaker to ensure a solvent saturated atmosphere throughout the drying process.

Characterization. Molar mass, composition, and polydispersity of the block copolymer were determined by a combination of gel permeation chromatography (GPC) and <sup>1</sup>H nuclear magnetic resonance (<sup>1</sup>H NMR) spectroscopy. SEM images were acquired using a Tescan LM Mira3 FE-SEM instrument with an in-lens detector (see Figure 2). For SAXS measurements, a small

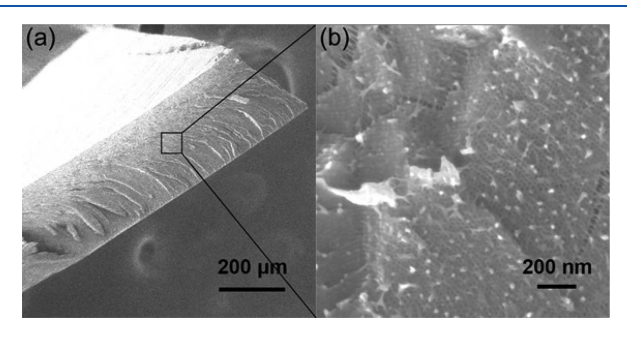


Figure 2. SEM images: (a) cross-section and (b) magnified images of bulk SI samples. Sample was about 200  $\mu$ m thick.

piece of bulk SI sample was placed in the hole of a metal washer that was covered on one side with Kapton tape. Transmission SAXS data were obtained at the G1 station of the Cornell High Energy Synchrotron Source (CHESS), with a sample-todetector distance of 2.02 m and an incident photon energy of 9.90 keV. Two-dimensional scattering patterns were recorded

on an Eiger 1 M pixel array detector (Dectris, Inc.) and radially integrated (see Figure 3). The spectra corresponded to a

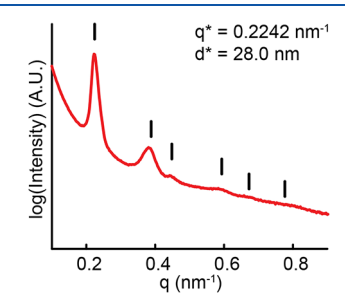
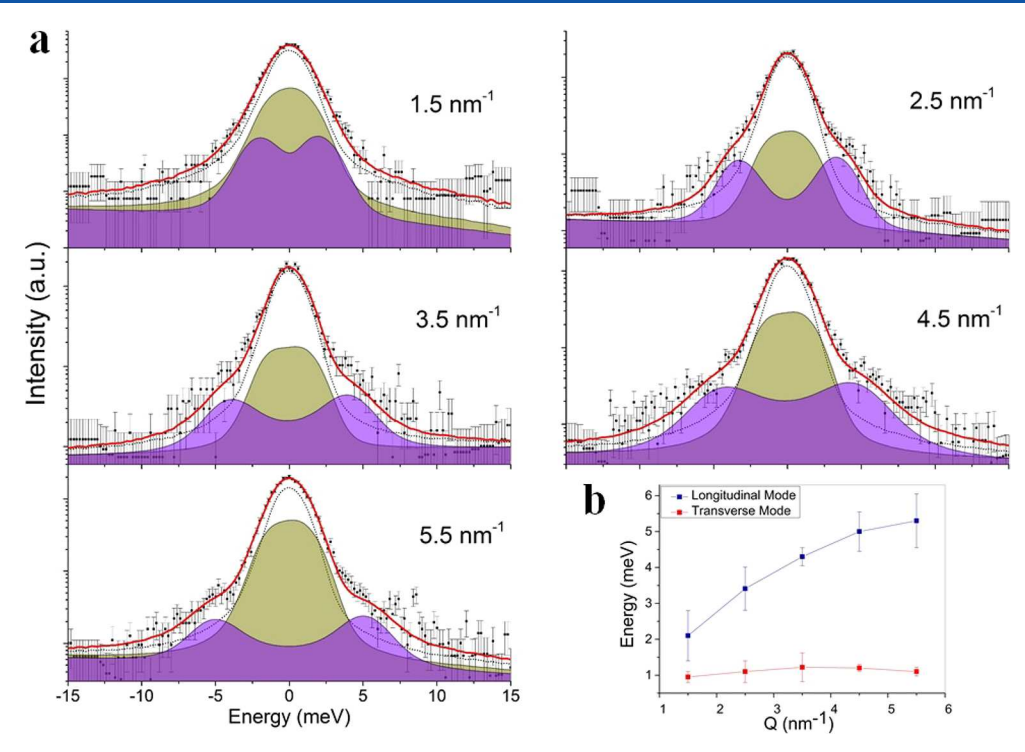


Figure 3. Radially integrated spectrum of the transmission SAXS pattern from the bulk SI sample. Peaks were indexed according to (q/q) $q^*)^2 = 1, 3, 4, 7, 9$ , and 12, consistent with a hexagonal lattice and also visible in the SEM image (see Figure 2b).

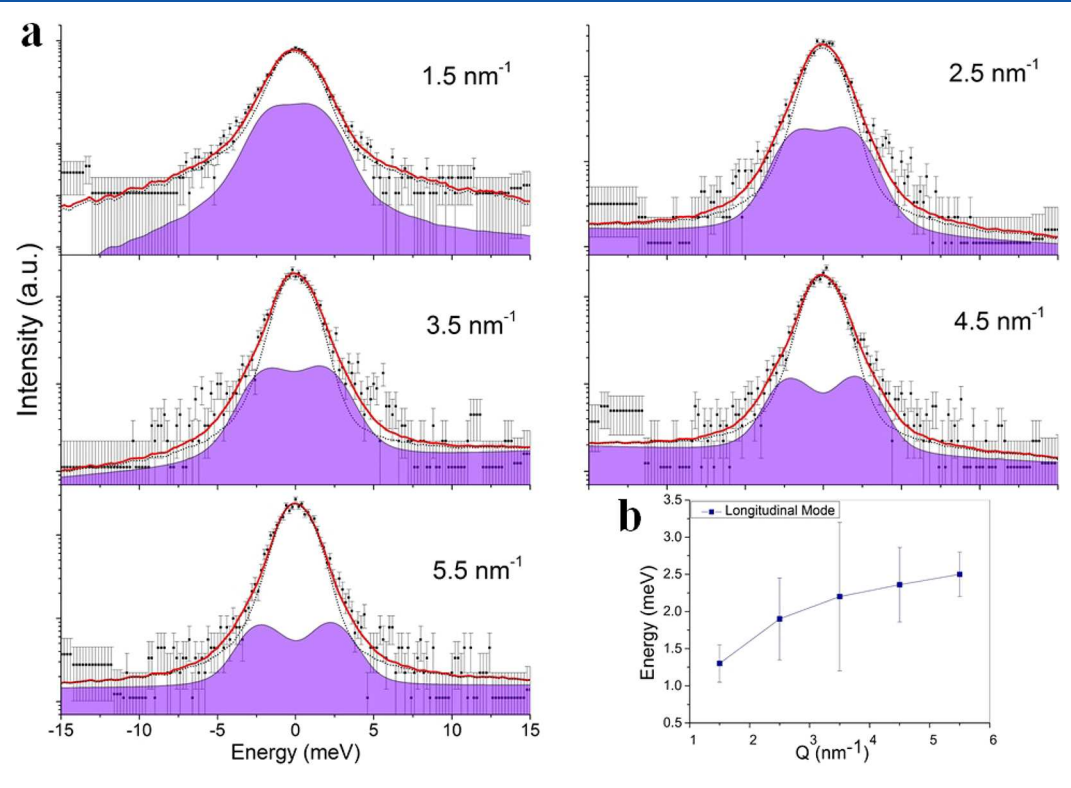
hexagonal lattice. To probe the Q-resolved phonon dynamics of the block copolymer we ran inelastic X-ray scattering measurements at the 10-ID beamline located at the National Synchrotron Light Source II (NSLS II), Brookhaven National Laboratory. The energy resolution function was nearly Gaussian in profile with a full width at half-maximum of  $\sim$ 2 meV. These data were key in identifying the various phonon modes. IXS measurements were carried out at an incident photon energy of 9.13 keV. A 10  $\times$  10  $\mu$ m<sup>2</sup> X-ray beam having a flux  $\sim$ 2  $\times$  10<sup>9</sup> photons/s impinged onto the sample. IXS energy scans were collected with Q-values between 1.5 and 5.5 nm<sup>-1</sup>, in 1 nm<sup>-1</sup> increments. A single IXS scan included 151 energy points with an acquisition time of 90 s per point. The scattering intensity was recorded in the horizontal plane within a 30 meV range; hence, only the van der Waals mediated phonon dynamics were probed, with the lateral planes of the polymer samples placed parallel to the scattering plane. The sample was translated across the beam at each scan to minimize beam damage.

Figure 4 shows IXS spectra and phonon dispersions of the bulk SI block copolymer at T = 30 °C. Apart from the observation of compression waves in the form of longitudinal phonons (blue line), we observed, for the first time, emergent shear elastic waves in the form of the transverse phonon mode (red line, see Figure 4b). A nearly Gaussian profile and the highspectral contrast of the resolution function were key factors in identifying both acoustic phonon modes in the framework of the damped harmonic oscillator (DHO) model.<sup>5</sup> The estimated longitudinal speed of sound in the bulk SI block copolymer is 1896 m/s, a value that is lower than the speed of sound in lamellar ordered styrene-b-(ethylene-alt-propylene) (SEP) diblock copolymers, i.e., 2040 m/s.<sup>64</sup> Moreover, the transverse phonon mode (see Figure 4b) barely disperses implying that it exists as a standing wave (breathing mode). In general, in soft materials, atoms/molecules within a unit cell can move with opposite phase to that of their neighbors. Such collective out-ofphase movements of atoms and molecules in opposite directions are called standing waves and show no dispersion near the long wavelength limit. The sound velocity of standing waves is nearly zero in the long wavelength implying that they simply do not propagate. Importantly, these standing waves can couple with light at corresponding energies/frequencies.

Figure 5 shows IXS spectra and phonon excitations in the bulk block copolymer at T = 90 °C, near its glass transition. At elevated temperatures, anharmonicity effects significantly affect the propagation of the elastic waves. The longitudinal phonon



**Figure 4.** Q-resolved phonon dynamics in bulk SI block copolymer at T = 30 °C: (a) IXS spectra of the bulk block copolymer sample. The experimental data are denoted by black squares, together with error bars, the resolution function (black dotted line), and the best least-squares fit (red solid curves) to the data. Low- and high-frequency damped harmonic oscillator (DHO) modes are denoted by the olive and purple solid curves with the filled areas, respectively. (b) Longitudinal acoustic (LA) and transverse acoustic (TA) phonon dispersion curves.



**Figure 5.** Q-resolved phonon dynamics in the bulk SI block copolymer at T = 90 °C: (a) IXS spectra of the bulk block copolymer sample. The notation is the same as in Figure 4. (b) The LA phonon branch is only observed. The TA mode became entirely extinct at 90 °C.

mode experiences a strong phonon attenuation, and the speed of sound drops down to 1365 m/s. Shear restoring forces at T=90 °C become negligibly weak resulting in the disappearance of low-energy transverse phonon excitations (Figure 5b). The

mechanism that is responsible for overdamping the transverse phonon modes is linked to anharmonicity effects due to the symmetry breaking in phonon interactions, which we elaborate below.

Anharmonicity-Mediated Symmetry Breaking Mechanism in Nanoscale Phonon Interactions. To understand the disappearance of the transverse phonon mode at T = 90 °C (see Figure 5) we will consider the following Hamiltonian:

$$H_{0} = \frac{1}{2} \sum_{0 \le \omega_{q} \le \omega_{D}} \left[ \prod_{q}^{\alpha} \prod_{-q}^{\alpha} + \mu \omega_{q}^{2} Q_{q}^{\alpha} Q_{-q}^{\alpha} - \frac{\sigma}{2} |Q_{q}^{\alpha}|^{4} + \frac{\theta}{6} |Q_{q}^{\alpha}|^{6} \right]$$
(1)

where  $\omega_q^2$  is the phonon dispersion relation, q is a multi-index  $\{q_1, q_2, q_3\}$ ,  $\alpha = (1, 2, 3)$ ,  $\omega_D$  is the Debye frequency, and  $\mu$ ,  $\sigma$ ,  $\theta \in \mathbb{R}^+$  are real non-negative couplings.  $Q_q^\alpha = \sqrt{m}\sum_{j=1}^N \mathrm{e}^{\mathrm{i}L(jq)}x_j^\alpha$  and  $\Pi_q^\alpha = \dot{Q}_q^\alpha$  are collective canonical coordinates, where  $x_j^\alpha$  is the space coordinate of an atom in a lattice sitting on a vertex labeled by the multi-index  $j = (j_1, j_2, j_3)$ , whose components span  $j_i \in (1, N_i)$ . The total number of atoms is  $N = N_1 N_2 N_3$ , i is the imaginary unit  $(\mathrm{i}^2 = -1)$ , and m is the mass of an atom in the lattice. The first term in eq 1 is the kinetic energy, and the remaining terms correspond to the potential energy which describes the interaction of phonons in reciprocal space. By varying the potential energy and considering the excitations of the phonon field around the ground state  $\bar{Q}_q^\alpha$  as  $Q_q^\alpha = \bar{Q}_q^\alpha + \varphi_q^\alpha$ , where  $\varphi_q^\alpha$  is the scalar field, for a chosen vacuum  $\bar{Q}_q^\alpha = \delta_1^\alpha |Q_q|$ , we obtain the effective Hamiltonian:

$$H[\varphi_{q}^{\alpha}] = \frac{1}{2} \sum_{0 \leq \omega_{q}^{l,t,t} \leq \omega_{D}} \pi_{q}^{l,t,t} \pi_{-q}^{l,t,t} + \sum_{0 \leq \omega_{q}^{l} \leq \omega_{D}} \left[ \frac{\omega_{q}^{2}}{2} \varphi_{q}^{l} \varphi_{-q}^{l} \right] + \sum_{\omega_{gap} \leq \omega_{q}^{t,t} \leq \omega_{D}} \left[ \frac{\omega_{q}^{2}}{2} (\varphi_{q}^{t} \varphi_{-q}^{t} + \varphi_{q}^{t} \varphi_{-q}^{t}) \right]$$
(2)

where  $\pi_q^{l,t,t}$  and  $\varphi_q^{l,t,t}$  are canonical coordinates, and l and t stand for the longitudinal and transverse phonon polarizations, respectively. The second term in eq 2 implies that longitudinal phonon excitations survive over the course of elevated anharmonic effects ( $0 \le \omega_q^{l,t,t} \le \omega_D$ ). In contrast, the transverse vibrations get overdamped due to anharmonicity-mediated<sup>67</sup> (potential energy in eq 1) symmetry breaking taking place in the nanoscale nonlinear phonon interactions, resulting in the extinction of the low-energy phonons<sup>68</sup> (see eq 2 and Figure 5). This implies that the  $\omega_{\rm gap}$  defines the minimal energy/frequency value for transverse phonons below which they do not get excited. However, the precise experimental determination of the  $\omega_{\mathrm{gap}}$  and  $Q_{\mathrm{gap}}$  through IXS will require experiments with finer Q-value steps that what was done presently. Additionally, the disappearance of transverse phonon excitations due to an anharmonicity-mediated mechanism, with increasing temperature, has been observed in soft and biological materials such as liquids, <sup>69,70</sup> liquid crystals, <sup>41,50</sup> lipid membranes, <sup>5</sup> and now in block copolymers. Recently, the emergence of the phonon gap in gel and liquid phospholipid membranes has been observed by D'Angelo et al., while stressing the role of the anharmonicitymediated mechanism.<sup>71</sup> In soft materials, increasing temperature results in longitudinal modes experiencing phonon attenuation, while transverse phonons do not experience this, even at supercritical thermodynamic conditions. 69,70

Block Polymer Thin Film Measurements. Synthesis of Poly(styrene-block-ethylene oxide) (SO) Polymerization. Benzene solvent was first distilled into a reactor situated in a glovebox, and the anionic initiator, sec-butyllithium (Sigma-Aldrich), was added to the reactor using a syringe. Styrene was distilled over di-n-butylmagnesium (Sigma-Aldrich), added to the reactor, and allowed to polymerize overnight. Then, 10×

moles of diphenylethylene (DPE, Sigma-Aldrich), relative to secbutyllithium, was then added to the reactor. Benzene was subsequently removed, and a similar amount of THF was distilled directly into the reactor. Ethylene oxide (EO) was kept between -20 and -10 °C, and distilled over n-butyllithium. Distilled EO was added into the reactor and stirred overnight. Equal moles of phosphazene base  $P_4$ -t-Bu and sec-butyllithium were then added to the reactor the next day. The reactor was subsequently heated up to 50 °C for 4 days, enabling EO to polymerize. Polymerization was stopped using degassed methanolic HCl. The block copolymer was dissolved in chloroform, washed against water 3 times, and precipitated into methanol.

Sample Preparation. First, a 5 wt % SI solution in THF was prepared and spin-coated on silicon substrates at a speed of 500 rpm for 1 min, as illustrated in Figure 1. The as-spun thin film has a thickness around 1  $\mu$ m, as shown in Figure 6c. The thin

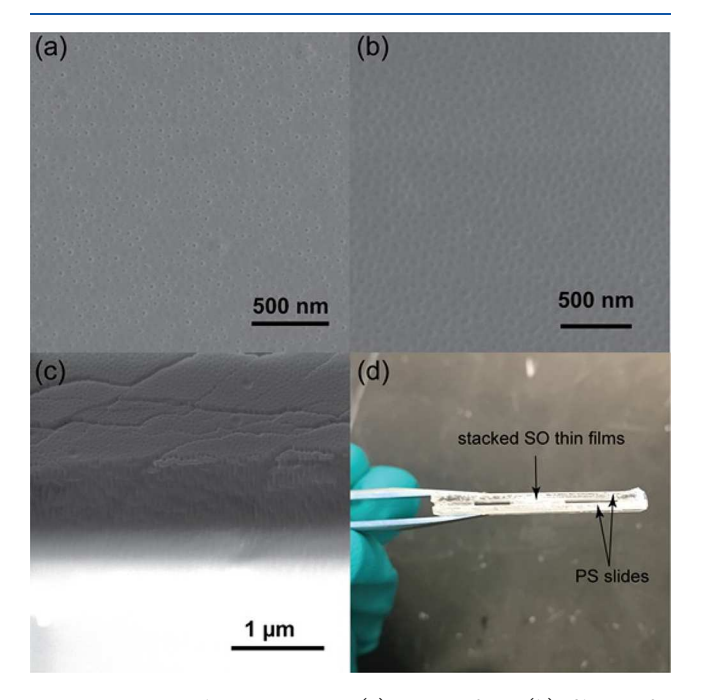


**Figure 6.** SEM characterization: (a) top surface, (b) film—wafer interface, and (c) cross-section of SO thin films prior to stacking. (d) Photo of SO thin films stacked to a thickness greater than 50  $\mu$ m and sandwiched between two polystyrene (PS) slides.

film was then solvent annealed (see the Methods section and the Supporting Information in ref 72). At the beginning, the flow rates of the dry and wet lines were set to 1.5 scfh (wet) and 0.1 scfh (dry) to solvent anneal the block copolymer thin film. After 10 min, the flow rates were readjusted to 0 scfh (wet) and 0.1 scfh (dry) to slowly deswell the thin films to their original thickness. SO thin films were then peeled off the Si wafer using a water bath. These free-standing thin films were then stacked (over 50 layers) and sandwiched between two polystyrene slides, as shown in Figure 6d. The polystyrene slides were then glued together at both ends with epoxy.

**Characterization.** SEM images were acquired using a Tescan LM Mira3 FE-SEM instrument with an in-lens detector. GISAXS patterns of SO thin films were collected prior to stacking (see Figure 7). Figure 8 shows IXS spectra and phonon dispersion curves of SO block copolymer films at T = 37 °C. The estimated longitudinal speed of sound in the SO thin film sample

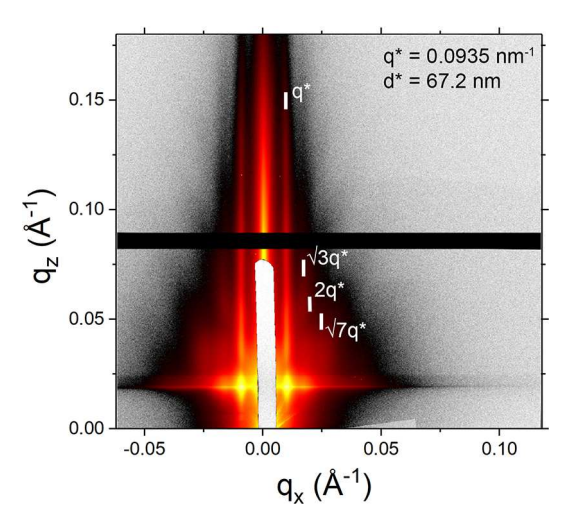


**Figure 7.** GISAXS pattern and associated indexing for the SO thin film prior to stacking. The indexing of the Bragg peaks is consistent with a hexagonal structure.

is 2275 m/s, which is consistent with a previously observed value. This value, however, is higher than that in the bulk SI sample (1896 m/s at T=30 °C) and that in lamellar ordered SEP diblock copolymers (2040 m/s at T=30 °C). Another common feature in the phonon spectra of soft materials, which was also observed in the present work, is the mixing of phonon polarizations due to anisotropic effects, which lead to nonlinear behavior of longitudinal phonons in the low-Q regime (see Figures 4b, 5b, and 8b). Such an effect is known as "positive sound" dispersion or "fast sound". Furthermore, the transverse phonon mode in SO thin films is equally non-dispersive, as is the case of the bulk SI sample which shows nearly zero slope toward the hydrodynamic limit ( $Q \rightarrow 0$ ) (see Figure 8), implying that transverse phonons do not propagate

but exist in the form of standing waves, mimicking optical phonons which are able to interact and couple with light at corresponding energies/frequencies. Indeed, soft materials such as liquids,  $^{74}$  DNA,  $^{75}$  lipid membranes,  $^{76}$  and, importantly, polymers,  $^{77}$  have been shown to absorb light in the 0.3–2.1 THz (1.2–8.7 meV) range, as revealed by far-IR and THz time domain spectroscopy (TDS).  $^{78}$  Moreover, recently IXS and THz TDS experiments have revealed that acoustic and optical phonon modes can coexist in nematic mesogens in a similar energy range, i.e.,  $\sim 1.5$  meV.  $^{50}$  Here, we provided compelling evidence for the existence of emergent transverse nonpropagating phonon modes (standing waves), both in bulk SI and SO thin film block copolymers. However, their ability to interact and possibly couple with THz light is yet to be directly observed, and could be an important development toward future THz optomechanical applications.

In this work, we studied Q-resolved nanoscale phonon dynamics in bulk SI and SO thin film block copolymers. The Qrange probed by IXS covers the first- and higher-order Brillouin zones, revealing the net vibrational properties of polymeric materials propagating over the PS matrix and PI/PO cylinderforming microphases. Their cylinder-forming hexagonally arranged static structures were characterized using SAXS and GISAXS, respectively, complemented by SEM measurements of their surface topography. We demonstrated that employing a cylinder-forming hexagonally arranged block copolymer structure is justified to study van der Waals mediated interchain Qresolved collective dynamics. Furthermore, an increase in temperature (from T = 30 to 90 °C) in the bulk SI block copolymer resulted in the disappearance of the shear interchain vibrational mode as a result of anharmonicity-mediated symmetry breaking in the nanoscale nonlinear phonon interactions. 66,68 The same effect has previously been observed experimentally in other soft materials. 5,43 Importantly, interest in the phonon dynamics of hexagonally arranged structures is

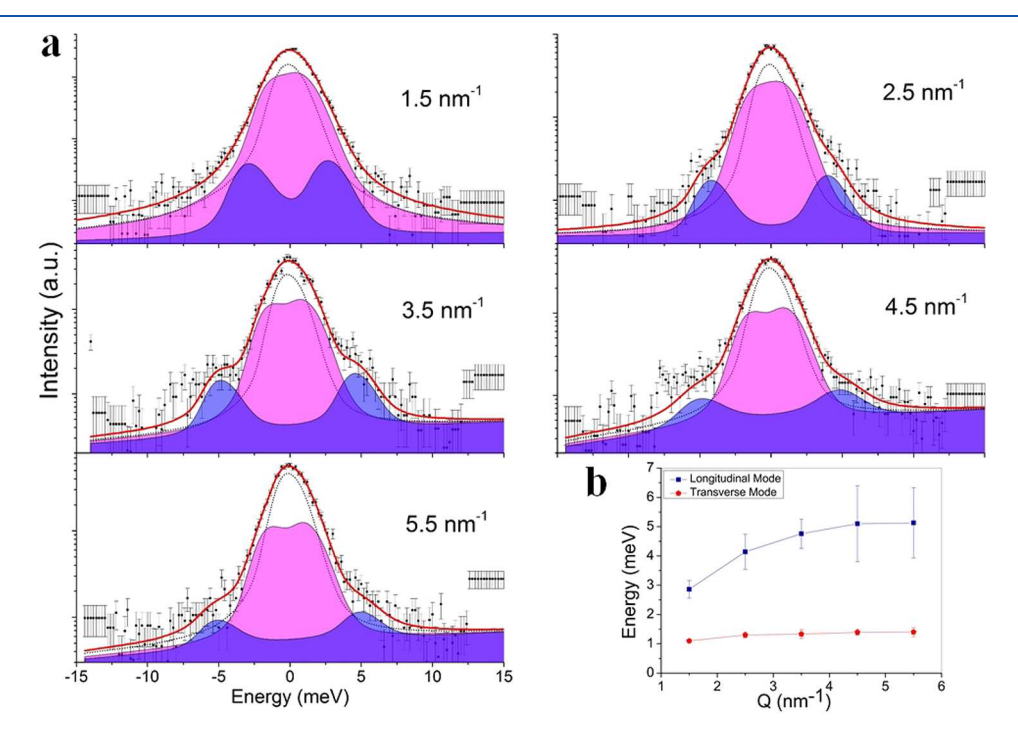


**Figure 8.** *Q*-resolved phonon dynamics in SO block copolymer films at T = 37 °C: (a) IXS spectra of the block copolymer film sample. Low- and high-frequency DHO modes are denoted by the magenta and blue solid curves with the filled areas, respectively. (b) LA and TA phonon excitations.

rapidly growing due to the observation of unique dispersion phenomena in the form of Dirac cones,<sup>79</sup> one-way edge phononic modes with topologically driven band gaps, topological boundary modes in isostatic lattices, 81 phonons<sup>82</sup> at high-symmetry points,<sup>83</sup> helical edge states in phononic topological insulators, 84 and topologically protected Weyl points. 85 Currently, it is challenging to study these phenomena in bulk SI and SO thin film block copolymers with IXS, due to the technique's limited spectral resolution. However, this obstacle may be overcome by reducing the size of the cylinders, and spacing them at distances comparable to the nanometer-wavelengths of THz phonons.

Finally, the detection of transverse phonon modes, both in bulk SI and SO thin film block copolymers, is of particular importance. As a proof of concept, we have demonstrated that these polymer compounds are dynamically responsive to Qresolved vibrational modes existing at the molecular level. Specifically, this type of polymeric material shows great promise for sensing molecular vibrations with nanoscale precision, especially at physiologically relevant conditions (T = 37 °C).

### AUTHOR INFORMATION

#### **Corresponding Author**

\*E-mail: d.bolmatov@gmail.com; bolmatovd@ornl.gov.

#### ORCID

Dima Bolmatov: 0000-0003-4179-8971 Qi Zhang: 0000-0001-5765-4505 Jörg G. Werner: 0000-0001-7845-086X Ulrich Wiesner: 0000-0001-6934-3755 Mikhail Zhernenkov: 0000-0003-3604-0672

#### **Notes**

The authors declare no competing financial interest.

## ACKNOWLEDGMENTS

We thank Jan-Michael Carrillo, Seung-Yeol Jeon, Kahyun Hur, Takeshi Egami, and Philip Pincus for fruitful discussions. J.K. is supported through the Scientific User Facilities Division of the Department of Energy (DOE) Office of Science, sponsored by the Basic Energy Science (BES) Program, DOE Office of Science, under Contract DEAC05-00OR22725. U.W. would like to thank the National Science Foundation for support (DMR-1707836). This work made use of the Cornell Center for Materials Research Shared Facilities, which are supported through the NSF MRSEC program (DMR-1719875), Cornell NanoScale Facility (CNF), a member of the National Nanotechnology Coordinated Infrastructure (NNCI), which is supported by the National Science Foundation (Grant ECCS-1542081), and the Cornell High Energy Synchrotron Source (CHESS), which is supported by the National Science Foundation under Award DMR-1332208. This research used IXS beamline (10-ID) of the National Synchrotron Light Source II, a U.S. Department of Energy (DOE) Office of Science User Facility operated for the DOE Office of Science by Brookhaven National Laboratory under Contract DE-SC0012704.

#### REFERENCES

- (1) Wang, X.; Zhu, X.; Chen, Y.; Zheng, M.; Xiang, Q.; Tang, Z.; Zhang, G.; Duan, H. Sensitive Surface-Enhanced Raman Scattering Detection Using On-Demand Postassembled Particle-on-Film Structure. ACS Appl. Mater. Interfaces 2017, 9 (36), 31102-31110.
- (2) Wang, H. W.; Chai, N.; Wang, P.; Hu, S.; Dou, W.; Umulis, D.; Wang, L. V.; Sturek, M.; Lucht, R.; Cheng, J. X. Label-Free Bond-

- Selective Imaging by Listening to Vibrationally Excited Molecules. Phys. Rev. Lett. 2011, 106, 238106.
- (3) Sun, K.; Huang, Q.; Meng, G.; Lu, Y. Highly Sensitive and Selective Surface-Enhanced Raman Spectroscopy Label-free Detection of 3,3',4,4'-Tetrachlorobiphenyl Using DNA Aptamer-Modified Ag-Nanorod Arrays. ACS Appl. Mater. Interfaces 2016, 8 (8), 5723-5728.
- (4) Atkin, J. M.; Sass, P. M.; Teichen, P. E.; Eaves, J. D.; Raschke, M. B. Nanoscale Probing of Dynamics in Local Molecular Environments. J. Phys. Chem. Lett. 2015, 6 (22), 4616-4621.
- (5) Zhernenkov, M.; Bolmatov, D.; Soloviov, D.; Zhernenkov, D.; Toperverg, K.; Cunsolo, B. P.; Bosak, A.; Cai, Y. Q. Revealing the Techanism of Passive Transport in Lipid Bilayers via Phonon-Mediated Nanometre-Scale Density Fluctuations. Nat. Commun. 2016, 7, 11575.
- (6) Gandman, A.; Mackin, R.; Cohn, B.; Rubtsov, I. V.; Chuntonov, L. Two-Dimensional Fano Lineshapes in Ultrafast Vibrational Spectroscopy of Thin Molecular Layers on Plasmonic Arrays. J. Phys. Chem. Lett. **2017**, 8 (14), 3341–3346.
- (7) Gao, Y.; Xu, B. Controllable Junction, In-Plane Heterostructures Capable of Mechanically Mediating On-Demand Asymmetry of Thermal Transports. ACS Appl. Mater. Interfaces 2017, 9 (39),
- (8) George, J.; Shalabney, A.; Hutchison, J. A.; Genet, C.; Ebbesen, T. W. Liquid-Phase Vibrational Strong Coupling. J. Phys. Chem. Lett. 2015, 6 (6), 1027–1031.
- (9) Li, M.; Xiao, Y.; Zhang, Z.; Yu, J. Bimodal Sintered Silver Nanoparticle Paste with Ultrahigh Thermal Conductivity and Shear Strength for High Temperature Thermal Material Applications. ACS Appl. Mater. Interfaces 2015, 7 (17), 9157-9168.
- (10) Chen, D.; Wan, Z.; Zhou, Y.; Zhou, X.; Yu, Y.; Zhong, J.; Ding, M.; Ji, Z. Dual-Phase Glass Ceramic: Structure, Dual-Modal Luminescence, and Temperature Sensing Behaviors. ACS Appl. Mater. Interfaces 2015, 7 (34), 19484-19493.
- (11) Bednarkiewicz, A.; Trejgis, K.; Drabik, J.; Kowalczyk, A.; Marciniak, L. Phosphor-Assisted Temperature Sensing and Imaging Using Resonant and Nonresonant Photoexcitation Scheme. ACS Appl. Mater. Interfaces 2017, 9 (49), 43081-43089.
- (12) Wang, P.; Rajian, J. R.; Cheng, J. X. Spectroscopic Imaging of Deep Tissue through Photoacoustic Detection of Molecular Vibration. J. Phys. Chem. Lett. 2013, 4 (13), 2177-2185.
- (13) Coskun, M. B.; Qiu, L.; Arefin, M. S.; Neild, A.; Yuce, M.; Li, D.; Alan, T. Detecting Subtle Vibrations Using Graphene-Based Cellular Elastomers. ACS Appl. Mater. Interfaces 2017, 9 (13), 11345-11349.
- (14) Taruttis, A.; Ntziachristos, V. Advances in Real-Time Multispectral Optoacoustic Imaging and Its Applications. Nat. Photonics 2015, 9, 219-227.
- (15) Dzierlenga, M. W.; Schwartz, S. D. Targeting a Rate-Promoting Vibration with an Allosteric Mediator in Lactate Dehydrogenase. J. Phys. Chem. Lett. 2016, 7 (13), 2591-2596.
- (16) Stuart, M. A. C.; Huck, W. T. S.; Genzer, J.; Muller, M.; Ober, C.; Stamm, M.; Sukhorukov, G. B.; Szleifer, I.; Tsukruk, V. V.; Urban, M. Emerging Applications of Stimuli-Responsive Polymer Materials. Nat. Mater. 2010, 9, 101-113.
- (17) Mohapatra, H.; Kim, H.; Phillips, S. T. Stimuli-Responsive Polymer Film that Autonomously Translates a Molecular Detection Event into a Macroscopic Change in Its Optical Properties via a Continuous, Thiol-Mediated Self-Propagating Reaction. J. Am. Chem. Soc. 2015, 137 (39), 12498-12501.
- (18) Ledin, P. A.; Jeon, J. W.; Geldmeier, J. A.; Ponder, J. F., Jr.; Mahmoud, M. A.; El-Sayed, M.; Reynolds, J. R.; Tsukruk, V. V. Design of Hybrid Electrochromic Materials with Large Electrical Modulation of Plasmonic Resonances. ACS Appl. Mater. Interfaces 2016, 8 (20), 13064-13075.
- (19) Shen, S.; Henry, A.; Tong, J.; Zheng, R.; Chen, G. Polyethylene Nanofibres with Very High Thermal Conductivities. Nat. Nanotechnol. 2010, 5 (4), 251-255.
- (20) Nunes, S. P.; Behzad, A. R.; Hooghan, B.; Sougrat, R.; Karunakaran, M.; Pradeep, N.; Vainio, U.; Peinemann, K. V. Switchable pH-Responsive Polymeric Membranes Prepared via Block Copolymer Micelle Assembly. ACS Nano 2011, 5 (5), 3516-3522.

- (21) He, X.; Aizenberg, M.; Kuksenok, O.; Zarzar, L. D.; Shastri, A.; Balazs, A. C.; Aizenberg, J. Synthetic Homeostatic Materials with Chemo-Mechano-Chemical Self-Regulation. *Nature* **2012**, *487*, 214–218
- (22) Hribar, K. C.; Lee, M. H.; Lee, D.; Burdick, J. A. Enhanced Release of Small Molecules from Near-Infrared Light Responsive Polymer-Nanorod Composites. *ACS Nano* **2011**, *5* (4), 2948–2956.
- (23) Cao, Y.; Liu, N.; Fu, C.; Li, K.; Tao, L.; Feng, L.; Wei, Y. Thermo and pH Dual-Responsive Materials for Controllable Oil/Water Separation. ACS Appl. Mater. Interfaces 2014, 6 (3), 2026–2030.
- (24) Cobo, I.; Li, M.; Sumerlin, B. S.; Perrier, S. Smart Hybrid Materials by Conjugation of Responsive Polymers to Biomacromolecules. *Nat. Mater.* **2015**, *14*, 143–159.
- (25) Thevenot, J.; Oliveira, H.; Sandre, O.; Lecommandoux, S. Magnetic Responsive Polymer Composite Materials. *Chem. Soc. Rev.* **2013**, *42*, 7099–7116.
- (26) Nakahata, M.; Takashima, Y.; Hashidzume, A.; Harada, A. Redox-Generated Mechanical Motion of a Supramolecular Polymeric Actuator Based on Host-Guest Interactions. *Angew. Chem., Int. Ed.* **2013**, *52*, *5731*–*5735*.
- (27) Tokarev, I.; Motornov, M.; Minko, S. Molecular-Engineered Stimuli-Responsive Thin Polymer Film: a Platform for the Development of Integrated Multifunctional Intelligent Materials. *J. Mater. Chem.* **2009**, *19*, 6932–6948.
- (28) Wojtecki, R. J.; Meador, M. A.; Rowan, S. J. Using the Dynamic Bond to Access Macroscopically Responsive Structurally Dynamic Polymers. *Nat. Mater.* **2011**, *10*, 14–27.
- (29) Ravula, T.; Ramadugu, S. K.; Mauro, G. D.; Ramamoorthy, A. Bioinspired, Size-Tunable Self-Assembly of Polymer-Lipid Bilayer Nanodiscs. *Angew. Chem., Int. Ed.* **2017**, *56*, 11466–11470.
- (30) Jiang, J.; Sherman, B. D.; Zhao, Y.; He, R.; Ghiviriga, I.; Alibabaei, L.; Meyer, T. J.; Leem, G.; Schanze, K. S. Polymer Chromophore-Catalyst Assembly for Solar. *ACS Appl. Mater. Interfaces* **2017**, 9 (23), 19529–19534.
- (31) Xu, Y.; Wang, X.; Zhou, J.; Song, B.; Jiang, Z.; Lee, E. M. Y.; Huberman, S.; Gleason, K. K.; Chen, G. Molecular Engineered Conjugated Polymer with High Thermal Conductivity. *Sci. Adv.* **2018**, *4*, eaar 3031.
- (32) Borodinov, N.; Gil, D.; Savchak, M.; Gross, C. E.; Yadavalli, N. S.; Ma, R.; Tsukruk, V. V.; Minko, S.; Vertegel, A.; Luzinov, I. En Route to Practicality of the Polymer Grafting Technology: One-Step Interfacial Modification with Amphiphilic Molecular Brushes. *ACS Appl. Mater. Interfaces* **2018**, *10* (16), 13941–13952.
- (33) Ribelli, T. G.; Fantin, M.; Daran, J. C.; Augustine, K. F.; Poli, R.; Matyjaszewski, K. Synthesis and Characterization of the Most Active Copper ATRP Catalyst Based on Tris[(4-dimethylaminopyridyl)-methyl]amine. J. Am. Chem. Soc. 2018, 140 (4), 1525–1534.
- (34) Tan, K. W.; Jung, B.; Werner, J. G.; Rhoades, E. R.; Thompson, M. O.; Wiesner, U. Transient Laser Heating Induced Hierarchical Porous Structures from Block Copolymer-Directed Self-Assembly. *Science* **2015**, 349, 54–58.
- (35) Yan, X.; Liu, Z.; Zhang, Q.; Lopez, J.; Wang, H.; Wu, H.-C.; Niu, S.; Yan, H.; Wang, S.; Lei, T.; et al. Quadruple H-Bonding Cross-Linked Supramolecular Polymeric Materials as Substrates for Stretchable, Antitearing, and Self-Healable Thin Film Electrodes. *J. Am. Chem. Soc.* **2018**, *140* (15), 5280–5289.
- (36) Robbins, S. W.; Beaucage, P. A.; Sai, H.; Tan, K. W.; Werner, J. G.; Sethna, J. P.; DiSalvo, F. J.; Gruner, S. M.; van Dover, R. B.; Wiesner, U. Block Copolymer Self-Assembly-Directed Synthesis of Mesoporous Gyroidal Superconductors. *Sci. Adv.* **2016**, *2*, e1501119.
- (37) Liu, D.; Chu, X. Q.; Lagi, M.; Zhang, Y.; Fratini, E.; Baglioni, P.; Alatas, A.; Said, A.; Alp, E.; Chen, S. H. Studies of Phononlike Low-Energy Excitations of Protein Molecules by Inelastic X-Ray Scattering. *Phys. Rev. Lett.* **2008**, *101*, 135501.
- (38) Zhao, D.; Schneider, D.; Fytas, G.; Kumar, S. K. Controlling the Thermomechanical Behavior of Nanoparticle/Polymer Films. *ACS Nano* **2014**, *8* (8), 8163–8173.
- (39) Bolmatov, D.; Zhernenkov, M.; Zav'yalov, D.; Cai, Y. Q.; Cunsolo, A. Terasonic Excitations in 2D Gold Nanoparticle Arrays in a

- Water Matrix as Revealed by Atomistic Simulations. J. Phys. Chem. C 2016, 120 (35), 19896–19903.
- (40) Kell, A.; Feng, X.; Reppert, M.; Jankowiak, R. On the Shape of the Phonon Spectral Density in Photosynthetic Complexes. *J. Phys. Chem. B* **2013**, *117* (24), 7317–7323.
- (41) Bolmatov, D.; Zhernenkov, M.; Sharpnack, L.; Agra-Kooijman, D. M.; Kumar, S.; Suvorov, A.; Pindak, R.; Cai, Y. Q.; Cunsolo, A. Emergent Optical Phononic Modes upon Nanoscale Mesogenic Phase Transitions. *Nano Lett.* **2017**, *17* (6), 3870–3876.
- (42) Li, M.; Chu, X. Q.; Fratini, E.; Baglioni, P.; Alatas, A.; Alp, E. E.; Chen, S. H. Phonon-Like Excitation in Secondary and Tertiary Structure of Hydrated Protein Powders. *Soft Matter* **2011**, *7*, 9848–9853.
- (43) Bolmatov, D.; Zhernenkov, M.; Zav'yalov, D.; Stoupin, S.; Cunsolo, A.; Cai, Y. Q. Thermally Triggered Phononic Gaps in Liquids at THz Scale. *Sci. Rep.* **2016**, *6*, 19469.
- (44) Gonzalez-Jimenez, M.; Ramakrishnan, G.; Harwood, T.; Lapthorn, A. J.; Kelly, S. M.; Ellis, E. M.; Wynne, K. Observation of Coherent Delocalized Phonon-Like Modes in DNA Under Physiological Conditions. *Nat. Commun.* **2016**, *7*, 11799.
- (45) Bolmatov, D.; Zhernenkov, M.; Zav'yalov, D.; Stoupin, S.; Cai, Y. Q.; Cunsolo, A. Revealing the Mechanism of the Viscous-to-Elastic Crossover in Liquids. J. Phys. Chem. Lett. 2015, 6 (15), 3048–3053.
- (46) Beltramo, P. J.; Schneider, D.; Fytas, G.; Furst, E. M. Anisotropic Hypersonic Phonon Propagation in Films of Aligned Ellipsoids. *Phys. Rev. Lett.* **2014**, *113*, 205503.
- (47) Bolmatov, D.; Brazhkin, V. V.; Trachenko, K. The Phonon Theory of Liquid Thermodynamics. Sci. Rep. 2012, 2, 421.
- (48) Frank, M.; Drikakis, D. Thermodynamics at Solid-Liquid Interfaces. *Entropy* **2018**, *20*, 362.
- (49) Schneider, D.; Gomopoulos, N.; Koh, C. Y.; Papadopoulos, P.; Kremer, F.; Thomas, E. L.; Fytas, G. Nonlinear Control of High-Frequency Phonons in Spider Silk. *Nat. Mater.* **2016**, *15*, 1079–1083.
- (50) Bolmatov, D.; Soloviov, D.; Zav'yalov, D.; Sharpnack, L.; Agra-Kooijman, D. M.; Kumar, S.; Zhang, J.; Liu, M.; Katsaras, J. Anomalous Nanoscale Optoacoustic Phonon Mixing in Nematic Mesogens. *J. Phys. Chem. Lett.* **2018**, *9* (10), 2546–2553.
- (51) Jang, J. H.; Ullal, C. K.; Gorishnyy, T.; Tsukruk, V. V.; Thomas, E. L. Mechanically Tunable Three-Dimensional Elastomeric Network/Air Structures via Interference Lithography. *Nano Lett.* **2006**, *6* (4), 740–743.
- (52) Mehra, N.; Mu, L.; Ji, T.; Li, Y.; Zhu, J. Moisture Driven Thermal Conduction in Polymer and Polymer Blends. *Compos. Sci. Technol.* **2017**, *151*, 115–123.
- (53) Maliakal, A. J. Characterization of Dopant Diffusion within Semiconducting Polymer and Small-Molecule Films Using Infrared-Active Vibrational Modes and Attenuated Total Reflectance Infrared Spectroscopy. ACS Appl. Mater. Interfaces 2013, 5 (17), 8300–8307.
- (54) Mu, L.; Ji, T.; Chen, L.; Mehra, N.; Shi, Y.; Zhu, J. Paving the Thermal Highway with Self-Organized Nanocrystals in Transparent Polymer Composites. *ACS Appl. Mater. Interfaces* **2016**, *8* (42), 29080–29087.
- (55) Mehra, N.; Li, Y.; Zhu, J. Small Organic Linkers with Hybrid Terminal Groups Drive Efficient Phonon Transport in Polymers. *J. Phys. Chem. C* **2018**, 122 (19), 10327–10333.
- (56) Li, Y.; Mehra, N.; Ji, T.; Yang, X.; Mu, L.; Gu, J.; Zhu, J. The Stiffness-Thermal Conduction Relationship at the Composite Interface: the Effect of Particle Alignment on the Long-Range Confinement of Polymer Chains Monitored by Scanning Thermal Microscopy. *Nanoscale* **2018**, *10*, 1695–1703.
- (57) Mu, L.; He, J.; Li, Y.; Ji, T.; Mehra, N.; Shi, Y.; Zhu, J. Molecular Origin of Efficient Phonon Transfer in Modulated Polymer Blends: Effect of Hydrogen Bonding on Polymer Coil Size and Assembled Microstructure. *J. Phys. Chem. C* **2017**, *121* (26), 14204–14212.
- (58) Alonso-Redondo, E.; Schmitt, M.; Urbach, Z.; Hui, C. M.; Sainidou, R.; Rembert, P.; Matyjaszewski, K.; Bockstaller, M. R.; Fytas, G. A New Class of Tunable Hypersonic Phononic Crystals Based on Polymer-Tethered Colloids. *Nat. Commun.* **2015**, *6*, 8309.

- (59) Mu, L.; Li, Y.; Mehra, N.; Ji, T.; Zhu, J. Expedited Phonon Transfer in Interfacially Constrained Polymer Chain Along Self-Organized Amino Acid. ACS Appl. Mater. Interfaces 2017, 9 (13), 12138–12145.
- (60) Mbarek, S.; Baroni, P.; Noirez, L. Highlighting Delayed Elastic Processes at Zero Stress in a Polymer Glass. *Polym. Int.* **2015**, *64*, 1303–1308.
- (61) Wunderlich, B. The Athas Database on Heat Capacities of Polymers. *Pure Appl. Chem.* **1995**, *67*, 1019–1026.
- (62) Tommaseo, G.; Penciu, R. S.; Fytas, G.; Economou, E. N.; Hashimoto, T.; Hadjichristidis, N. Phonon Propagation in Ordered Diblock Copolymer Solutions. *Macromolecules* **2004**, 37 (13), 5006–5010.
- (63) Noirez, L.; Baroni, P. Identification of Thermal Shear Bands in a Low Molecular Weight Polymer Melt Under Oscillatory Strain Field. *Colloid Polym. Sci.* **2018**, 296, 713–720.
- (64) Kriegs, H.; Steffen, W.; Fytas, G.; Monaco, G.; Dreyfus, C.; Fragouli, P.; Pitsikalis, M.; Hadjichristidis, N. High Frequency Acoustic Excitations in Ordered Diblock Copolymer Studied by Inelastic X-Ray Scattering. *J. Chem. Phys.* **2004**, *121*, 2376.
- (65) Kim, G. H.; Lee, D.; Shanker, A.; Shao, L.; Kwon, M. S.; Gidley, D.; Kim, J.; Pipe, K. P. High Thermal Conductivity in Amorphous Polymer Blends by Engineered Interchain Interactions. *Nat. Mater.* **2015**, *14*, 295–300.
- (66) Bolmatov, D.; Zav'yalov, D.; Zhernenkov, M.; Musaev, E. T.; Cai, Y. Q. Unified Phonon-Based Approach to The Thermodynamics of Solid, Liquid and Gas States. *Ann. Phys.* **2015**, 363, 221–242.
- (67) Henry, A.; Chen, G.; Plimpton, S. J.; Thompson, A. 1D-to-3D Transition of Phonon Heat Conduction in Polyethylene Using Molecular Dynamics Simulations. *Phys. Rev. B: Condens. Matter Mater. Phys.* **2010**, 82, 144308.
- (68) Bolmatov, D.; Musaev, E. T.; Trachenko, K. Symmetry Breaking Gives Rise to Energy Spectra of Three States of Matter. *Sci. Rep.* **2013**, 3, 2794.
- (69) Bolmatov, D.; Zhernenkov, M.; Zav'yalov, D.; Stoupin, S.; Cunsolo, A.; Cai, Y. Q. Thermally Triggered Phononic Gaps in Liquids at THz Scale. *Sci. Rep.* **2016**, *6*, 19469.
- (70) Bolmatov, D.; Zhernenkov, M.; Zav'yalov, D.; Stoupin, S.; Cai, Y. Q.; Cunsolo, A. Revealing the Mechanism of the Viscous-to-Elastic Crossover in Liquids. *J. Phys. Chem. Lett.* **2015**, *6*, 3048–3053.
- (71) D'Angelo, G.; Nibali, V. C.; Wanderlingh, U.; Branca, C.; Francesco, A.; Sacchetti, F.; Petrillo, C.; Paciaroni, A. Multiple Interacting Collective Modes and Phonon Gap in Phospholipid Membranes. *J. Phys. Chem. Lett.* **2018**, *9* (15), 4367–4372.
- (72) Zhang, Q.; Matsuoka, F.; Suh, H. S.; Beaucage, P. A.; Xiong, S.; Smilgies, D. M.; Tan, K. W.; Werner, J. G.; Nealey, P. F.; Wiesner, U. B. Pathways to Mesoporous Resin/Carbon Thin Films with Alternating Gyroid Morphology. *ACS Nano* **2018**, *12* (1), 347–358.
- (73) Cang, Y.; Reuss, A. N.; Lee, J.; Yan, J.; Zhang, J.; Alonso-Redondo, E.; Sainidou, R.; Rembert, P.; Matyjaszewski, K.; Bockstaller, M. R. Thermomechanical Properties and Glass Dynamics of Polymer-Tethered Colloidal Particles and Films. *Macromolecules* **2017**, *50* (21), 8658–8669.
- (74) Das Mahanta, D.; Samanta, N.; Mitra, S. K. The Effect of Monovalent Cations on the Collective Dynamics of Water and on a Model Protein. *J. Mol. Liq.* **2016**, *215*, 197–203.
- (75) Tang, M.; Huang, Q.; Wei, D.; Zhao, G.; Chang, T.; Kou, K.; Wang, M.; Du, C.; Fu, W. L.; Cui, H. L. Terahertz spectroscopy of oligonucleotides in aqueous solutions. *J. Biomed. Opt.* **2015**, *20*, 095009.
- (76) D'Angelo, G.; Nibali, V. C.; Crupi, C.; Rifici, S.; Wanderlingh, U.; Paciaroni, A.; Sacchetti, F.; Branca, C. Probing Intermolecular Interactions in Phospholipid Bilayers by Far-Infrared Spectroscopy. *J. Phys. Chem. B* **2017**, *121* (6), 1204–1210.
- (77) Serin, G.; Nguyen, H. H.; Marty, J. D.; Micheau, J. C.; Gernigon, V.; Mingotaud, A. F.; Bajon, D.; Soulet, T.; Massenot, S.; Coudret, C. Terahertz Time-Domain Spectroscopy of Thermoresponsive Polymers in Aqueous Solution. *J. Phys. Chem. B* **2016**, *120* (36), 9778–9787.

- (78) El Khoury, Y.; Hellwig, P. Far Infrared Spectroscopy of Hydrogen Bonding Collective Motions in Complex Molecular Systems. *Chem. Commun.* **2017**, *53*, 8389–8399.
- (79) Kariyado, T.; Hatsugai, Y. Manipulation of Dirac Cones in Mechanical Graphene. *Sci. Rep.* **2016**, *5*, 18107.
- (80) Wang, P.; Lu, L.; Bertoldi, K. Topological Phononic Crystals with One-Way Elastic Edge Waves. *Phys. Rev. Lett.* **2015**, *115*, 104302.
- (81) Kane, C. L.; Lubensky, T. C. Topological Boundary Modes in Isostatic Lattices. *Nat. Phys.* **2014**, *10*, 39–45.
- (82) Xu, X.; Zhang, W.; Wang, J.; Zhang, L. Topological Chiral Phonons in Center-Stacked Bilayer Triangle Lattices. *J. Phys.: Condens. Matter* **2018**, 30, 225401.
- (83) Zhang, L.; Niu, Q. Chiral Phonons at High-Symmetry Points in Monolayer Hexagonal Lattices. *Phys. Rev. Lett.* **2015**, *115*, 115502.
- (84) Susstrunk, R.; Huber, S. D. Observation of Phononic Helical Edge States in a Mechanical Topological Insulator. *Science* **2015**, 349, 47–50
- (85) Fruchart, M.; Jeon, S. Y.; Hur, K.; Cheianov, V.; Wiesner, U.; Vitelli, V. Soft Self-Assembly of Weyl Materials for Light and Sound. *Proc. Natl. Acad. Sci. U. S. A.* **2018**, *115*, E3655—E3664.